Bioselection of a Gain of Function Mutation that Enhances Adenovirus 5 Release and Improves Its Antitumoral Potency

Alena Gros, Jordi Martínez-Quintanilla, Cristina Puig, Sonia Guedan, David G. Molleví, Ramon Alemany, and Manel Cascallo

Translational Research Laboratory, IDIBELL-Institut Català d'Oncologia, L'Hospitalet de Llobregat, Barcelona, Spain

Abstract

Genetic bioselection of a mutagenized Ad5wt stock in human tumor xenografts led us to isolate AdT1, a mutant displaying a large-plaque phenotype *in vitro* and an enhanced systemic antitumor activity *in vivo*. AdT1 phenotype correlates with an increased progeny release without affecting total viral yield in different human tumors and cancer-associated fibroblasts. An approach combining hybrid Ad5/AdT1 recombinants and sequencing identified a truncating insertion in the endoplasmic reticulum retention domain of the E3/19K protein (445A mutation) which relocates the protein to the plasma membrane and is responsible for AdT1's enhanced release. E3/19K-445A phenotype does not correlate with the protein's ability to interact with MHC-I or induce apoptosis. Intracellular calcium measurement revealed that the 445A mutation induces extracellular Ca^{2+} influx, deregulating intracellular Ca^{2+} homeostasis and inducing membrane permeabilization, a viroporin-like function. E3/19K-445A mutants also display enhanced antitumoral activity when injected both intratumorally and systemically in different models *in vivo*. Our results indicate that the inclusion of mutation 445A in tumor-selective adenoviruses would be a very powerful tool to enhance their antitumor efficacy. [Cancer Res 2008;68(21):8928–37]

Introduction

Tumor-selective viruses are being engineered to treat cancer (1). Different strategies have been used to render adenovirus tumor specific (2). Results to date have shown a good security/toxicity profile for multiple modes of delivery. Flu-like symptomatology has been reported as the most common toxicity, especially after i.v. delivery, along with transient transaminitis and, occasionally, thrombocytopenia (3). Antitumor effects have also been described after intratumoral or intracavital injection, and the potential for synergy with chemotherapy is very promising (4). However, systemic antitumoral response rates range only from minimal to moderate after systemic administration (5, 6).

One of the reasons that explain the poor response to oncolytic adenovirus after i.v. administration is the biodistribution profile of adenovirus 5 (Ad5), a non–blood-borne virus that is quickly cleared from the bloodstream after i.v. administration and accumulates in the liver within minutes due to the particular hepatic architecture and vascular system (7, 8). The presence of the host immune system may also be determinant in the response to oncolytic adenoviruses, although its exact role is not clear, with some discrepancies between preclinical data and clinical results (9, 10). In addition, other biological barriers within the tumor mass (for example, the tumor stroma matrix) also limits adenovirus oncolysis by hindering the spread of the virions (11, 12).

Improving adenovirus potency has been postulated as an important step to overcome all these limitations (13). One approach to render adenoviruses more cytotoxic is arming oncolytic adenoviruses with transgenes that are able to eliminate surrounding cells and favor spreading of the oncolytic effect. With this aim, several proteins have been incorporated into the adenovirus backbone, including the adenovirus death protein (14), p53 (15), different prodrug-converting enzymes (16), and immunomodulators (17). Although successful results have been obtained with some of these constructs, the utility of this strategy has been often limited by the small cloning capacity of most oncolytic adenoviruses after the insertion of the genetic elements required to confer selectivity.

Bioselection of randomly mutagenized adenovirus by repeated passaging in defined conditions can also be used as a strategy for the isolation of mutants that exhibit potent and/or tumor-selective phenotypes. This genetic selection has the potential to assign novel functions to viral genes. For example, new mutants of human Ad5 with enhanced oncolytic activity were isolated after repeated passage of a randomly mutagenized pool in a human colorectal cancer cell line *in vitro* (18). A point mutation that induced a COOH terminal truncation in the i-leader protein, resulting in its early accumulation, was shown to be essential for the mutant phenotype (18). Interestingly, the relevance of such mutations in the i-leader protein has been further confirmed by another study (19).

With the aim of selecting Ad5 mutants with enhanced antitumor activity, we have extended the genetic selection approach by including the *in vivo* tumor environment as selective pressure. A mutant isolated from tumors, AdT1, displayed an increased antitumor activity *in vivo* and large-plaque phenotype *in vitro*. Further characterization showed that AdT1 presented an improved viral release without affecting the overall yield in both human tumor cells and cancer-associated fibroblasts. A combined approach including sequencing and analysis of recombinants revealed that the presence of a mutation in the endoplasmic reticulum retention domain of the E3/19K protein was responsible for the phenotype. We propose that the expression of the mutated form of E3/19K is able to disturb intracellular Ca^{2+} homeostasis and ultimately create membrane lesions that allow enhanced virus release.

Materials and Methods

Cell lines and viruses. Human HEK293, A549, FaDu, SKMel-28, and NP-9 (20) cell lines and hamster pancreatic tumor HP-1 cells (21) were grown in

Note: Supplementary data for this article are available at Cancer Research Online (http://cancerres.aacrjournals.org/).

Requests for reprints: Manel Cascallo, IDIBELL-Institut Català d'Oncologia, Av Gran Via s/n km 2,7, L'Hospitalet de Llobregat, 08907 Barcelona, Spain. Phone: 34-93-2607463; Fax: 34-93-2607466; E-mail: mcascallo@iconcologia.net.

doi:10.1158/0008-5472.CAN-08-1145

DMEM supplemented with 5% fetal bovine serum (FBS). CAF1 cells, human carcinoma-associated fibroblasts, were isolated and characterized in our laboratory from an hepatic metastasis of a human colorectal carcinoma and were maintained in DMEM-F12 supplemented with 10% FBS and BD MITO$^+$ serum extender (Becton Dickinson). When evaluating effects of extracellular Ca^{2+}, CAF1 cells were seeded in fibronectin-coated dishes. To obtain >80% infection, 293, A549, FaDu, DLD-1, SKMel-28, NP-9, CAF1 and HP-1 cells were infected with 5, 20, 25, 15, 25, 30, 45, and 50 transducing units (TU) per cell, respectively. As calcium-containing medium, a Ca^{2+}-free medium to which $CaCl_2$ was added to a final concentration of 1.8 mmol/L was used. Calcium-free medium was supplemented with 0.5 mmol/L EGTA immediately before use. Human Ad5 was obtained from American Type Culture Collection (ATCC). AdTL (AdGFPLuc) has been previously described (22). Oligonucleotides were designed to sequence Ad5 and AdT1 entire viral genomes.

Random mutagenesis and *in vivo* selection. An Ad5 stock was randomly mutagenized with nitrous acid (23) and the 8 min–treated stock (1,000-fold loss of virus viability; average of nine mutations per genome) was chosen for the first round of *in vivo* selection. Mutations were fixed, and the mutagenized stock was subsequently amplified and purified by passage at a high TU per cell in A549 cells to prevent *in vitro* selection of mutants. For each round of *in vivo* selection, 1×10^7 NP-9 cells were injected s.c. into the flanks of male BALB/c *nu/nu* mice. Animal studies were performed in the IDIBELL facility (AAALAC unit 1155) and approved by the IDIBELL's Ethical Committee for Animal Experimentation. Once the tumors reached 100 mm^3, mice were injected with PBS, Ad5, or the mutagenized Ad5 stock at 2×10^{10} vp by tail vein. At 4 h postinjection, blood was drawn from the tail and the titer was determined by an anti-hexon staining method. Body weights of the animals were monitored, and tumor volume was calculated as previously described (11). The virus mutants with superior blood persistence were amplified from a blood sample of the mouse that displayed the best tumor growth inhibition and were chosen for the next round of *in vivo* selection. After the fourth round of bioselection, the virus mutants were extracted from the tumor that showed the most pronounced tumor growth inhibition. The AdT1 mutant was isolated from the resulting tumor cell lysate by plaque assay in A549 cells.

Construction of Ad5/AdT1 recombinants and E3/19K modified viruses. Homologous recombination for the generation of modified viruses was performed in yeast. The yeast replication elements and a selectable marker were cloned into pAd5 plasmid (ref. 24; pAd5CAU). Homologous recombination between different fragments of pAd5CAU and AdT1 genome (represented schematically in Fig. 2*A*) resulted in the generation of the different Ad5/AdT1 recombinants used to map the mutation(s) responsible for the large-plaque phenotype of AdT1. Plasmids pAdE3/19K-445A, pAdE3/19K-445ACS40, pAdE3/19K-KS, pAdE3/19K-CS40, and pAdE3/19K-del (Supplementary Table S1) were constructed by recombination of pAd5CAU with PCR-modified E3/19K sequences, and the incorporated modifications were sequenced. Viruses were generated in 293, propagated in A549, and quantified using the anti-hexon staining–based method using 293 cells (24). Briefly, this method consists in the infection of 293 cells with serial dilutions of a virus sample. Thirty-six hours postinfection, cells were fixed with methanol and incubated with mouse anti-hexon (2Hx-2 hybridoma, ATCC) and Alexa 488–labeled goat anti-mouse (Molecular Probes) during 1 h at 37°C. The similar late protein expression pattern showed by the viruses (Supplementary Fig. S2*B*) assured this method was suitable for the titration of the mutant viruses generated.

Virus release and production assays. 293, A549, CAF1, NP-9, FaDu, SkMel-28, DLD-1, or HP-1 cells were infected to allow 80% to 100% infection. Three hours later, infection medium was removed and cells were washed twice with PBS and incubated with fresh medium. At the indicated time points a fraction of the supernatant (SN) and the cell-media suspension (CE) were harvested. Viral titers were determined in triplicate according to an anti-hexon staining–based method, as described above. For experiments in which the effects of extracellular calcium were assayed, cells were infected, and medium was removed 24 h later, the cells were washed twice with PBS (-$CaCl_2$/-$MgCl_2$) and subsequently incubated with normal or Ca^{2+}-free medium.

***In vitro* cytotoxicity assay.** Cytotoxity assay was performed by seeding 30,000 A549 cells, 10,000 NP-9 cells, or 50,000 DLD-1 cells per well in 96-well plates in DMEM with 5% FBS. Cells were infected with serial dilutions starting with 90 TU/cell for A549, 250 TU/cell for NP-9, and 20 TU/cell for DLD-1 cells. At day 5 postinfection, plates were washed with PBS and stained for total protein content (bicinchoninic acid assay, Pierce Biotechnology) and absorbance was quantified. The TU per cell required to produce 50% inhibition (IC_{50} value) was estimated from dose-response curves by standard nonlinear regression (GraFit; Erithacus Software), using an adapted Hill equation.

Western blot analysis. A549 cells were either mock-infected or infected to allow >80% infection, and protein cell extracts were prepared 24 h postinfection with Iso-Hi-pH buffer [0.14 mol/L NaCl, 1 mmol/L $MgCl_2$, 10 mmol/L Tris-HCl (pH 8.5), 0.5% Nonidet P-40]. Protein samples (20 μg/lane) were separated by SDS/PAGE and transferred to membranes. Blots were probed with the following antibodies: anti-E3/19K (ref. 25; Tw1.3 that recognizes a luminal epitope of the protein kindly provided by Dr. Yewdell, NIAID/NIH), anti-E1A (clone 13S-5, Santa Cruz Biotechnology), anti-Ad5 virion proteins (ab6982, Abcam), anti-human poly(ADP-ribose) polymerase (PARP; clone 551024, Becton Dickinson), or anti-adenovirus death protein (ADP; specific for residues 63–77 of the Ad2 ADP sequence kindly provided by Dr. W.S.M. Wold, St. Louis University; ref. 26).

E3/19K and MHC-I membrane expression analysis by fluorescence-activated cell sorting. Cell surface expression of E3/19K and MHC class I in virus-infected cells was analyzed in A549 cells using anti-E3/19K (Tw1.3) and anti-human MHC-I (W6/32, ATCC), respectively. Twenty-four hours postinfection, fluorescence profiles were obtained in triplicate by analyzing 10,000 viable cells by flow cytometry (FACSCalibur, Becton Dickinson) using 488-nm laser and CellQuest Pro software (Becton Dickinson).

Propidium iodide uptake and measurement of intracellular Ca^{2+} concentration. A549 or CAF1 monolayers were infected to obtain 80% infection. Cells were harvested at various times postinfection. For permeability studies, suspensions were incubated with 1 μg/mL propidium iodide (PI; Bender Medsystems) for 15 min at room temperature. The number of permeable cells was determined in triplicate by flow cytometry (FACSCalibur, Becton Dickinson). To determine intracellular Ca^{2+} concentration, cells were incubated with 10 μmol/L Fluo-3 acetoxymethyl ester (AM) and 20 μmol/L Fura-red AM (Invitrogen) indicators, as previously described (27). The loaded A549 cells were analyzed in triplicate by flow cytometry (FACSCalibur, Becton Dickinson).

Evaluation of antitumor efficacy *in vivo*. Pancreatic human NP-9 tumor xenografts were established s.c. into the flanks of BALB/c *nu/nu* mice as described above. To evaluate systemic efficacy of the viruses carrying E3/19K-445A mutation, mice with 100 mm^3 tumors (n = 10 per group) were treated with a single i.v. injection of PBS, Ad5, AdT1, or AdE3/19K-445A (2×10^{10} vp/mouse in 150 μL PBS). The VP/TU ratio of the purified virus stocks used for the *in vivo* efficacy experiments was similar as shown in Supplementary Table S2. To evaluate intratumoral efficacy, 100 mm^3 tumors (n = 10 per group) were treated with a single intratumoral injection of PBS, Ad5, AdT1, or AdE3/19K-445A (2×10^9 vp/tumor in 25 μL PBS). To evaluate the efficacy of E3/19K-445A mutants in an immune competent model, HP-1 tumors were induced in the flanks of female 5-wk-old immune competent Syrian (golden) hamsters (*Mesocricetus auratus*) by s.c. inoculation of 1×10^6 cells. Once tumors reached 150 to 170 mm^3, hamsters were randomized (n = 10 per group), and a single intratumoral injection was performed with Ad5 or AdT1 at 2.5×10^{10} vp/tumor in 25 μL PBS or with PBS. In each model, tumor sizes and animal body weights were recorded and tumor volume and growth were calculated according to the corresponding formulas. The two-tailed Student's t test was used for comparing the tumor progression in mice in the different treatment groups.

Intratumoral adenovirus detection. Adenovirus immunofluorescence in hamster tumors was performed as previously described (24). Briefly, OCT-embedded sections from HP-1 tumors obtained at day 29 after virus administration were treated with polyclonal anti-adenovirus (clone Ab6982, Abcam Ltd.) and Alexa Fluor 488–labeled goat anti-rabbit (Molecular Probes) antibodies and counterstained with 4′,6-diamino-2-phenylindole. Stained slides were analyzed under a fluorescent microscope (Olympus BX51).

Results

***In vivo* bioselection of Ad5 mutants with enhanced oncolytic efficacy.** A purified stock of wild-type human Ad5 was randomly mutated with nitrous acid as previously described (23). The mutagenized stock was amplified in human lung adenocarcinoma A549 cells and subjected to various rounds of selection *in vivo* in BALB/c *nu/nu* mice harboring s.c. human pancreatic NP-9 tumors to select mutants with improved oncolytic potency (see Materials and Methods). In the fourth round of bioselection, the virus mutants were extracted from the tumor that showed the most pronounced growth inhibition and plaque-purified to isolate clones. One of these clones, AdT1, was further characterized, and the mutations responsible for its phenotype are the main focus of this study.

Characterization of the phenotype of AdT1. To compare the systemic antitumor efficacy of Ad5 and AdT1, mice with s.c. NP-9 tumors were treated with a single i.v. dose of 2×10^{10} vp and the tumor growth was monitored. Mutant AdT1 showed an enhanced antitumor activity compared with Ad5 (Fig. 1*A*), and this correlated with intratumoral viral replication (not shown).

The enhanced antitumor efficacy displayed by AdT1 *in vivo* was associated with a large-plaque phenotype *in vitro* (Fig. 1*B*). The plaques of AdT1 in A549 cells appeared earlier and were at least twice as large as the control Ad5 plaques. The AdT1 large-plaque phenotype could result from an increase in the viral yield or an increase in viral release. The measurement of intracellular and extracellular virus in A549 cells showed that AdT1 was released more efficiently from infected cells, whereas the total virus produced was unaffected (Fig. 1*C*). Because fibroblasts release adenovirus less efficiently than epithelial cells and are relevant target cells in oncolysis of tumors with stroma, we analyzed and confirmed the enhanced release of AdT1 in carcinoma-associated fibroblasts (CAF1; Fig. 1*C*). This increase in the rate of viral release was also observed in 293 cells and human tumor cell lines from head and neck (FaDu), melanoma (SkMel-28), pancreas (NP-9), and colorectal carcinoma (DLD-1), as well as in hamster pancreatic tumor HP-1 cells (Fig. 1*D*), confirming that this phenotype was not restricted to the cells used during the bioselection process. The enhanced release also resulted in an

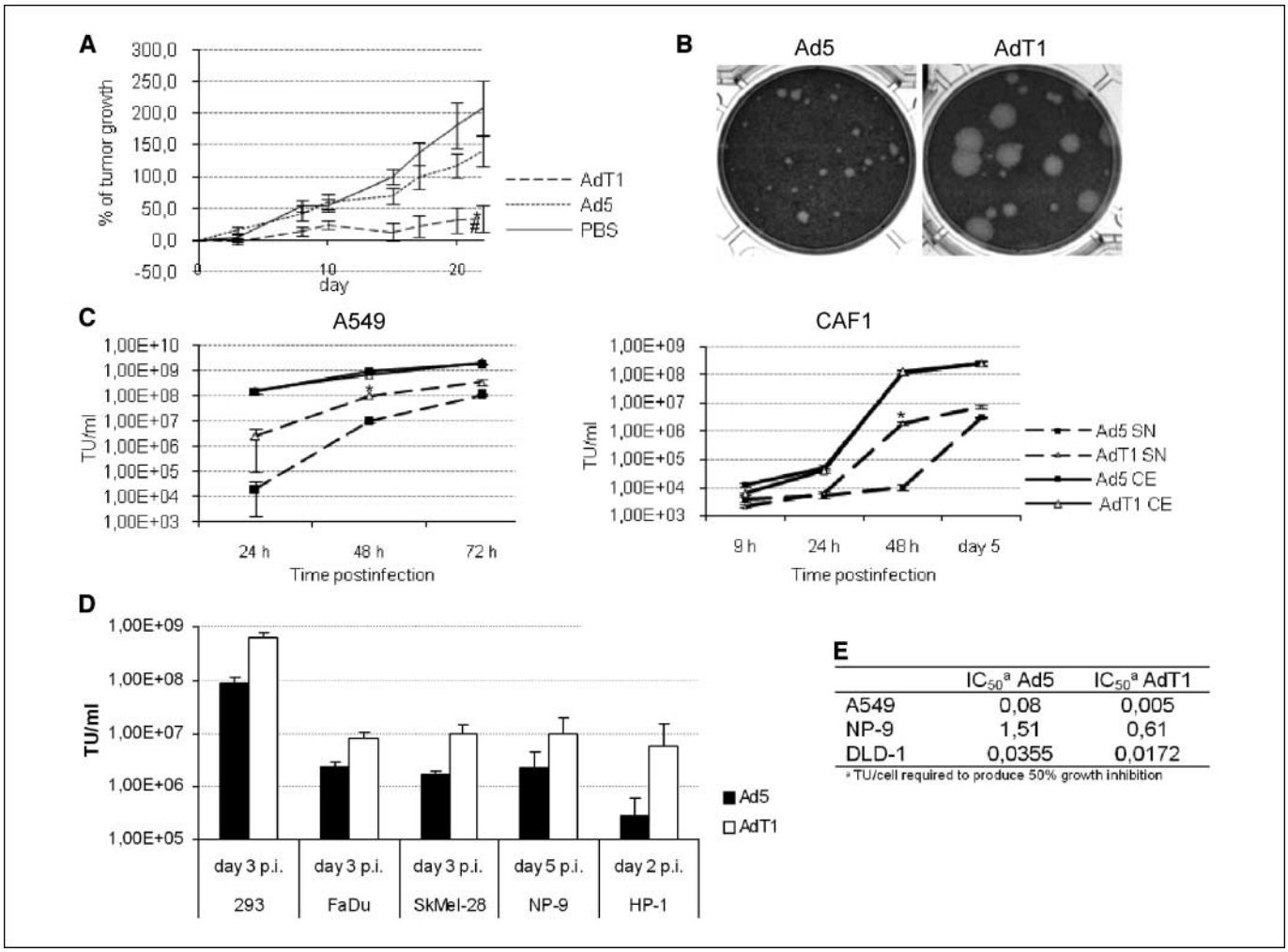

E

	IC_{50}[a] Ad5	IC_{50}[a] AdT1
A549	0,08	0,005
NP-9	1,51	0,61
DLD-1	0,0355	0,0172

[a] TU/cell required to produce 50% growth inhibition

Figure 1. Characterization of the phenotype of AdT1. *A,* NP-9 tumor xenografts were treated i.v. with PBS, Ad5, or AdT1. *Points,* mean percentage of tumor growth ($n = 10$); *bars,* SE. #, significant ($P = 0.03$) compared with the group treated with PBS; *, significant ($P = 0.03$) compared with mice injected with Ad5. *B,* plaque size of Ad5 and AdT1 in A549 cells at day 7 postinfection. *C,* viral production and release kinetics of Ad5 and AdT1 in A549 cells (*left*) and carcinoma-associated fibroblasts (CAF1 cells; *right*). Extracellular (SN) and intracellular (CE) viral content were analyzed at the time points indicated. *, significant ($P = 8.9e{-}05$ and $P = 0.01$ for A549 and CAF1 cells, respectively) compared with Ad5. *D,* viral release of Ad5 and AdT1 in a panel of different tumor cell lines. Titer of the supernatant at the time point at which AdT1 and Ad5 showed biggest differences for each cell line. *E,* comparative cytotoxicity of Ad5 and AdT1 in A549, NP-9, and DLD-1 tumor cell lines.

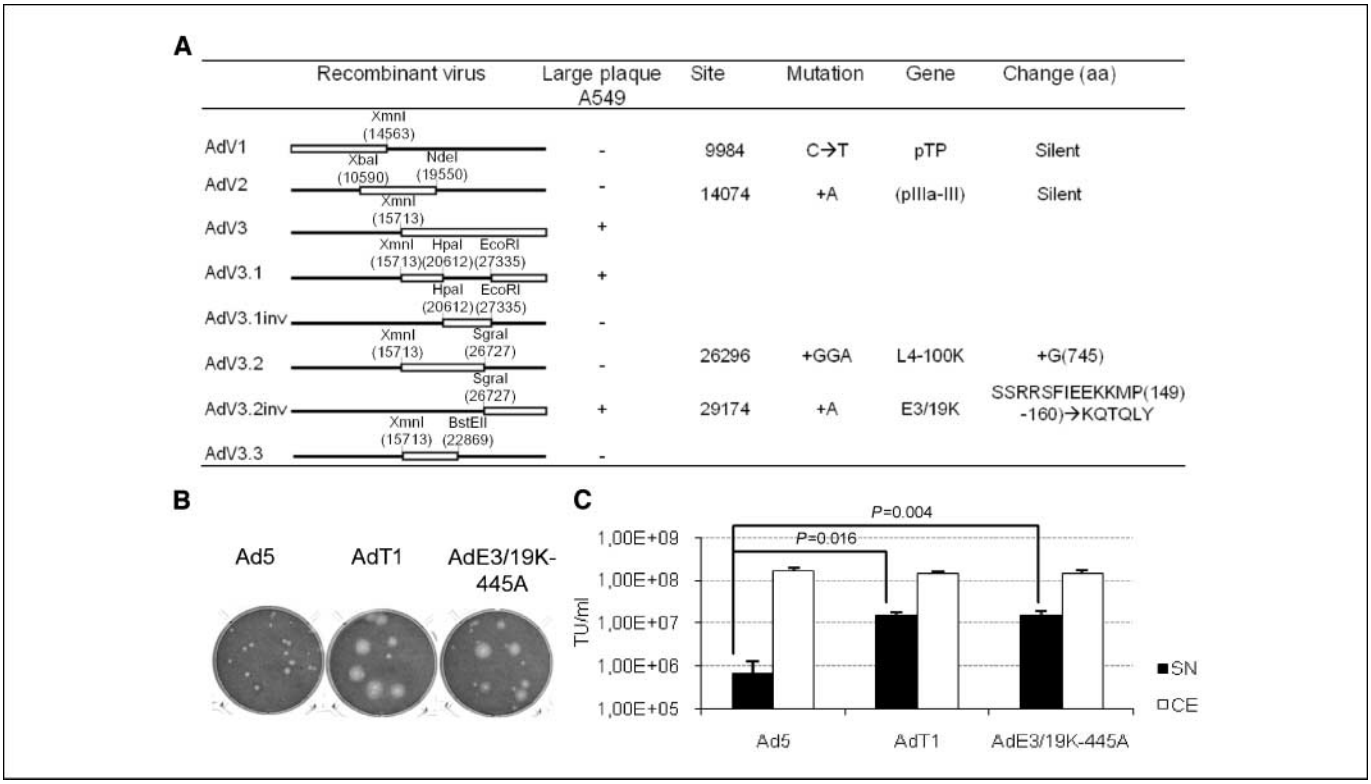

Figure 2. Identification of the mutations responsible for the AdT1 phenotype. *A,* schematic representation of the Ad5/AdT1 recombinants and the mutations present in the AdT1 genome. The fragments of the Ad5 (*black*) and AdT1 (*white*) genomes and the enzymes used for the construction of the recombinants are represented, as well as their ability to form large plaques in A549 monolayers. The site and genes affected by the mutations are specified. Nucleotide changes (→) and insertions (+) are indicated. Mutations located between two protein coding regions are indicated in parentheses. *pTP,* preterminal protein. The amino acid (*aa*) positions affected by the mutation are indicated in parentheses. *B,* plaque morphology of Ad5, AdT1 and AdE3/19K-445A in A549 cells 7 d after infection. *C,* viral release and production of Ad5, AdT1, and AdE3/19K-445A in carcinoma-associated fibroblasts. CAF1 cells were infected, and virus present in the supernatant (SN) and cell extract (CE) was measured 48 h postinfection.

enhanced cytotoxicity, as tested in A549, NP-9, and DLD-1 cells (Fig. 1*E*). The dominance of the phenotype of AdT1 was confirmed by performing a cell-plaque assay after coinfection with a GFP-expressing E1A-deleted adenoviral vector (Supplementary Fig. S1).

Identification of the mutation(s) responsible for the enhanced viral release of AdT1: E3/19K-445A mutation. We carried out the functional mapping of the AdT1 phenotype and complete sequence analysis of AdT1 genome. The Ad5/AdT1 recombinants mapped the mutation responsible for the large-plaque phenotype to nucleotides 27335 to 35935 of AdT1 (schematically represented in Fig. 2*A*). The sequence analysis of the genome revealed four mutations (Fig. 2*A*). Among these, two were silent and one inserted three nucleotides (GGA) in position 26296 of Ad5, which introduced an extra Gly at position 745 of the amino acid sequence of the L4-100K protein. The fourth mutation, found in position 29174, inserted an adenine into position 445 of the nucleotide sequence of the E3/19K protein. Because mutation E3/19K-445A was the only change detected in the smallest fragment of AdT1 that was able to confer large-plaque phenotype, we hypothesized it was responsible for the phenotype. The generation of mutant AdE3/19K-445A proved that this mutation was sufficient to enhance the release of Ad5. This mutation conferred both a large-plaque phenotype in A549 (Fig. 2*B*) and an enhanced viral release without modifying the viral yield in CAF1 cells (Fig. 2*C*). With these data, we concluded that mutation E3/19K-445A was responsible for the enhanced release observed with AdT1.

The change in localization of the E3/19K protein enhances adenovirus release. E3/19K protein is a small glycoprotein coded by the early region E3 of Ad5. The cytoplasmic tail of this protein, affected by mutation E3/19K-445A, contains a dilysine motif essential for the retention of E3/19K in the endoplasmic reticulum (ER; refs. 25, 28). Mutation E3/19K-445A generates a shift in the open reading frame (ORF) that changes the amino acid sequence from position 149 and generates a stop codon at position 154. As a result, E3/19K-445A presents a truncated cytoplasmic tail, which results in the loss of the ER retention signal and is expected to relocalize E3/19K to the plasma membrane.

The enhanced viral release observed with AdE3/19K-445A could be due to the loss of function of the E3/19K protein or to the gain of function of this protein when translocated to the cell surface. Two viruses were constructed to test this hypothesis: AdE3/19K-del, which lacks E3/19K expression (nucleotides 28846–29201 of Ad5 were deleted), and AdE3/19K-KS, a mutant different from AdE3/19K-445A which also affects the ER retention domain of this protein (the dilysine motif was substituted for two serines, KK→SS; ref. 29; Supplementary Table S1). As Fig. 3*A* displays, cell surface expression of the E3/19K was only detected in the cells infected with the viruses that had lost the ER retention signal: AdT1, AdE3/19K-445A, and AdE3/19K-KS. The lack of E3/19K expression in mutant AdE3/19K-del was confirmed by Western blot, as shown in

Fig. 3*B*. Interestingly, a viral release assay in CAF1 cells showed that AdE3/19K-KS was released 100 times more efficiently than Ad5 (Fig. 3*C*). The phenocopy of AdT1 and AdE3/19K-445A by AdE3/19K-KS established a direct association between the change of localization of E3/19K and the enhanced rate of viral release and suggested a new function for E3/19K at the cell membrane. By contrast, AdE3/19K-del showed levels of extracellular virus comparable with Ad5, in concordance with previous studies stating that the lack of E3/19K expression does not increase adenovirus release (30).

The enhanced release phenotype of mutant AdE3/19K-445A is not mediated by interaction with MHC-I at the cell surface or by apoptosis. The main function of E3/19K is to bind to and retain the heavy chains of MHC class I in the ER, preventing CTL response against adenoviral infection (25, 28, 31). Consequently, the loss of ER retention of E3/19K-445A inhibits ER retention of MHC-I. We hypothesized that the interaction of E3/19K and MHC-I at the plasma membrane could be triggering the enhanced release observed with AdE3/19K-445A. For this purpose, we constructed mutant AdE3/19K-445ACS40, which contained both the E3/19K-445A mutation and the substitution of a cysteine in position 40 of the amino acid sequence of E3/19K for a serine (C→S-40), which prevents MHC-I binding (32). As Fig. 4*A* displays, the analysis of cell surface expression of MHC-I showed that AdE3/19K-445A blocked MHC-I transport to the plasma membrane less efficiently, although it did not reach basal levels of MHC-I expression, as previously described (33). On the other hand, mutant AdE3/19K-445ACS40 showed similar cell surface MHC-I expression as the uninfected cells. This confirms that this mutant is unable to prevent MHC-I transport to the membrane, because it is unable to bind to MHC-I (significant differences compared with AdE3/19K-445A). A viral release assay in CAF1 cells showed that, although AdE3/19K-445ACS40 was unable to bind to MHC-I, it was released earlier into the supernatant (Fig. 4*B*). This mutant also displayed a large-plaque phenotype in A549 (Supplementary Table S1), proving that the phenotype was not dependent on interaction with MHC-I. Additional evidence suggesting that the AdT1 mutant did not enhance viral release by interacting with MHC-I comes from the enhanced release phenotype of AdT1 in a cell line negative for MHC-I expression, such as DLD-1 (Fig. 1*D* and Supplementary Table S1).

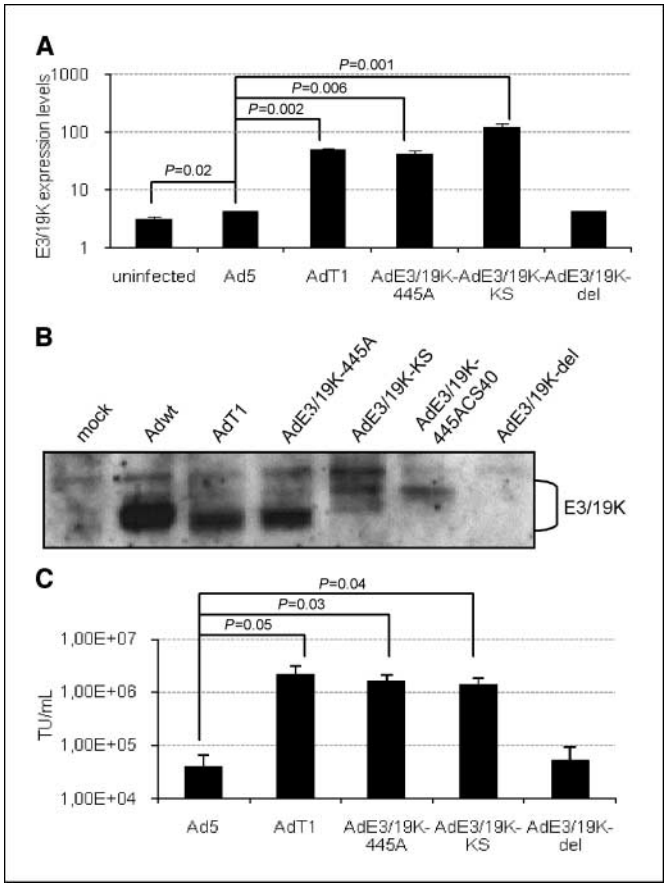

Figure 3. Association of E3/19K localization to the plasma membrane and the phenotype of enhanced release. *A,* cell surface expression of E3/19K protein in A549 cells. Expression of E3/19K in the plasma membrane was analyzed at 24 h postinfection in nonpermeabilized cells by flow cytometry with Tw1.3 antibody. *B,* Western blot detection of E3/19K. A549 cell lysates were processed for E3/19K protein expression 24 h postinfection with the adenovirus mutants indicated. *C,* viral release of Ad5, AdT1, AdE3/19K-445A, AdE3/19K-KS, and AdE3/19K-del in carcinoma-associated fibroblasts. Virus present in the supernatant was measured 48 h postinfection in CAF1.

Adenovirus mutants defective in viral genes that inhibit apoptosis produce a characteristic phenotype similar to that observed with AdT1 and AdE3/19K-445A (34).To determine the levels of apoptosis activation with our mutants, we analyzed PARP cleavage during the viral cycle. As Fig. 4*C* displays, the level of PARP cleavage in AdT1 and AdE3/19K-445A–infected cells was similar to that seen for Ad5, which shows that these mutants were unable to activate apoptosis. Further confirmation of the apoptosis independence of the AdE319K-445A phenotype was gained from viral release experiments in CAF1 cells treated with the broad spectrum caspase inhibitor Q-VD-OPh. Both the viral release and plaque-size of AdE3/19K-445A were not affected by the presence of Q-VD-OPh, proving that the enhanced rate of viral release was not mediated by apoptosis (Fig. 4*D*; Supplementary Table S1).

The enhanced release of E3/19K-445A–expressing mutants is not mediated by ADP overexpression. ADP is a small glycoprotein coded by the E3 region of Ad5 required for the efficient lysis of adenovirus-infected cells. Its overexpression results in an enhanced release and large-plaque phenotype (14, 30, 35). The expression of this protein is tightly regulated by pre-mRNA processing and some deletion mutations upstream of ADP which affect splicing or polyadenylation sites increase the expression of its early transcripts (26, 36). The proximity of E3/19K and ADP ORF led us to study a possible ADP overexpression caused by the E3/19K-445A mutation. No differences were found in the pattern of E3 transcripts (Supplementary Fig. S2*A*). Early ADP transcripts (bands *d* and *e*) were not detected 8 hours postinfection for neither Ad5 nor AdT1 but were greatly amplified 24 hours postinfection (bands *d*′ and *e*′), as previously described (26). Western blot detection of ADP expression in the different mutants confirmed these results and dismissed ADP overexpression in AdT1 and AdE3/19K-445A–infected cells (Supplementary Fig. S2*B*). Furthermore, no differences in E1A nor adenovirus late protein expression were found for the different virus mutants (Supplementary Fig. S2*B*).

Mutant AdE3/19K-445A enhances cell permeability and increases intracellular [Ca^{2+}]. Some viruses actively enhance cell permeability during viral infection by the expression of viroporins, facilitating the influx of extracellular ions, which can enhance viral release through yet unknown mechanisms (37, 38). To study a putative viroporin-like function of E3/19K-445A, we analyzed cell permeability and intracellular Ca^{2+} concentration throughout the viral cycle. AdE3/19K-445A enhanced cell permeability at earlier

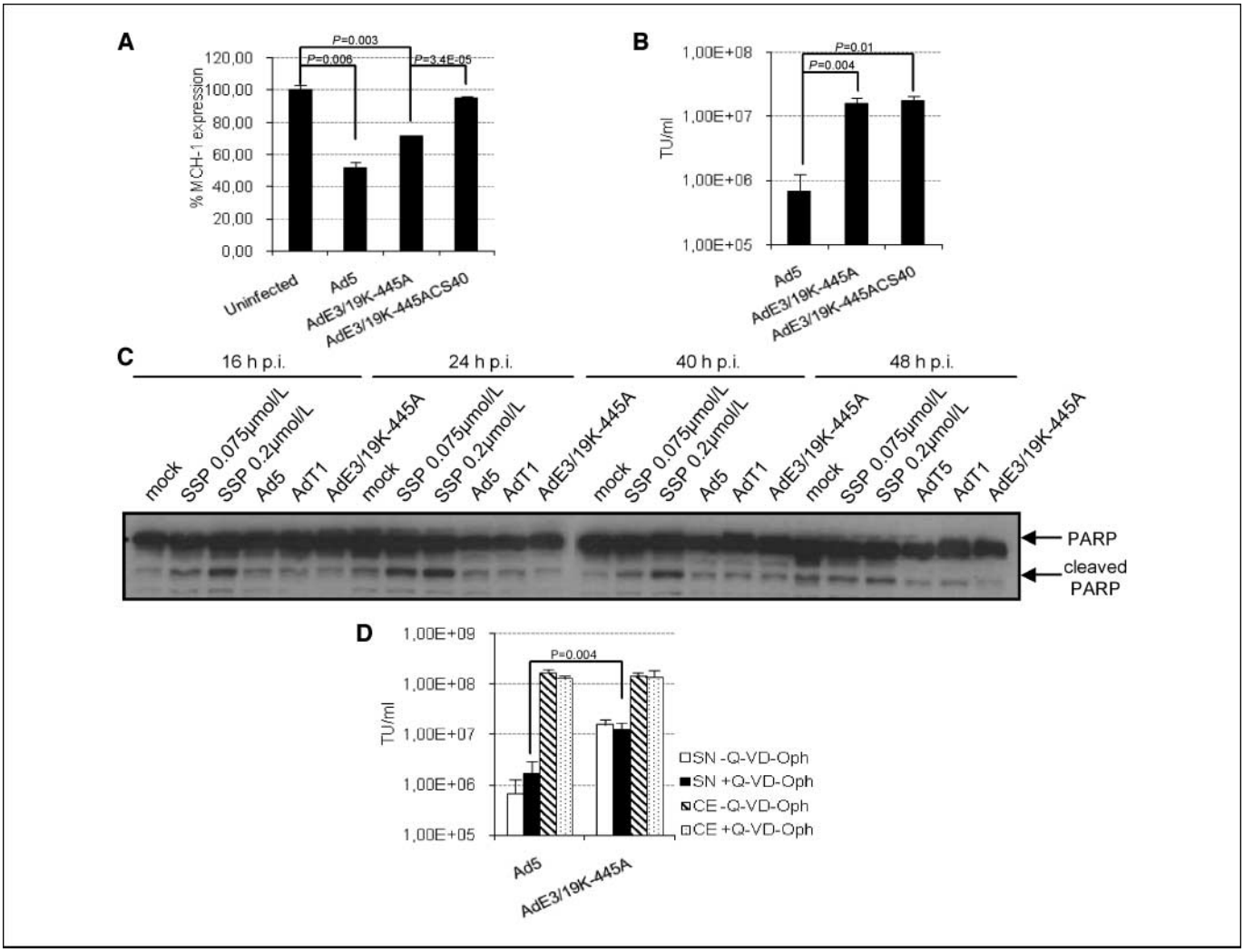

Figure 4. MHC-I binding and apoptosis independence of the enhanced release phenotype of AdT1. *A,* fluorescence-activated cell sorting analysis of MHC-I cell surface expression in mutant and Ad5-infected human A549 cells. Cells were infected and, 24 h later, exposed to the monoclonal antibody W6/32. Cell surface levels of class I antigens are expressed relative to that of mock-infected cells, which were set to 100%. *B,* viral release assay of Ad5, AdE3/19K-445A, and AdE3/19K-445ACS40 in carcinoma-associated fibroblasts. Cells were infected, and the virus present in the supernatant (SN) was measured 48 h postinfection. *C,* Western blot detection of PARP cleavage in mutant and Ad5-infected A549 cells. Mock-infected cells or infected with Ad5, AdT1, or AdE3/19K-445A or treated with 0.075 μmol/L and 0.2 μmol/L of staurosporine (*SSP*) as a positive control of apoptosis induction were analyzed. The cell lysates were processed for detection of PARP cleavage at 16, 24, 40, and 48 h postinfection. *D,* viral release and production of Ad5 and AdE3/19K-445A in carcinoma-associated fibroblasts in the presence of a broad spectrum apoptosis inhibitor, Q-VD-Oph. Cells were infected and incubated in the presence or absence of 20 μmol/L Q-VD-Oph. The extracellular (SN) and intracellular (CE) viral content was measured 48 h postinfection.

stages of infection (Fig. 5*A*), and this increase in cell permeability was associated with an increase in the intracellular Ca^{2+} concentration (Fig. 5*B*). This enhanced permeability for AdE3/19K-445A–infected cells was also observed in CAF1 (Fig. 5*C*). To test whether the influx of Ca^{2+} was the cause of the enhanced rate of viral release, we performed a viral release and production assay in CAF1 cells in the presence or absence of extracellular Ca^{2+}. Although the lack of Ca^{2+} in the extracellular medium affected the viral yield of both viruses, the differences in viral release between Ad5 and AdE3/19K-445A disappeared in the absence of Ca^{2+} (Fig. 5*D*), proving that the enhanced release of AdE3/19K-445A was triggered, at least in part, by Ca^{2+} influx.

Evaluation of *in vivo* efficacy. Mice carrying NP-9 pancreatic tumors were treated with a single i.v. dose of Ad5 or AdE3/19K-445A at 2×10^{10} vp/mouse. The enhanced antitumor activity shown by AdE3/19K-445A compared with Ad5 proves that the 445A mutation is not only responsible for the enhanced release and cytotoxicity of AdT1 *in vitro* but also for the gain of oncolytic effect *in vivo* (Fig. 6*A*). In a second model, we assessed the comparative *in vivo* efficacy of Ad5, AdT1, and AdE3/19K-445A with a single intratumoral injection of virus into NP-9 s.c. tumors. Even in such conditions, in which we potentiate the amount of Ad5 in the tumor, both the AdT1 and AdE3/19K-445A–treated tumors responded better with respect to Ad5 (Fig. 6*B*). We also performed a third *in vivo* experiment in Syrian hamsters that has been described as an immunocompetent model wherein human adenovirus is able to replicate (Fig. 6*C*). Hamsters with s.c. pancreatic HP-1 tumors were treated intratumorally at a dose of 2.5×10^{10} vp/tumor. Both Ad5 and AdT1 displayed significant antitumoral activity, although no statistical significance among these groups was observed. Analysis of HP-1 tumor sections revealed that despite the presence of extensive areas of necrosis in all experimental groups, tumors

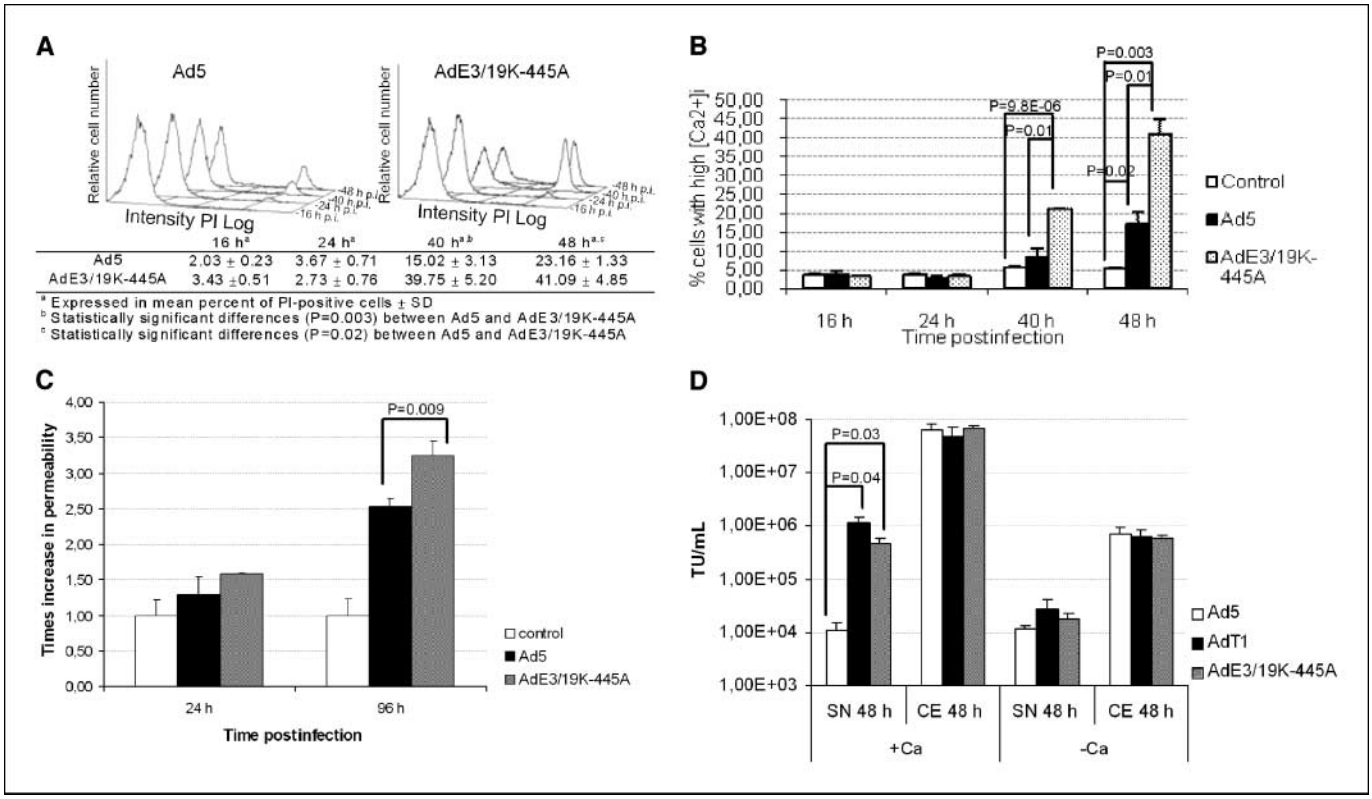

Figure 5. Adenovirus mutant AdE3/19K-445A enhances membrane permeabilization and increases intracellular Ca^{2+} concentration. *A,* kinetics of cell permeability of Ad5-infected and AdE3/19K-445A–infected A549 cells. Cells were infected and, at the indicated time points, trypsinized and incubated with PI. The number of permeable cells (PI-positive cells) was determined. The intensity of PI for infected cells is represented in a logarithmic scale. *B,* kinetics of cytosolic free Ca^{2+} during Ad5 and AdE3/19K-445A infection. A549 cells infected with Ad5 or AdE3/19K-445A were incubated at the indicated time points with Fluo-3 AM and Fura-red AM. The Fluo-3/Fura-red ratio for each cell was analyzed, and cells were divided into a population with a high ratio (high intracellular [Ca^{2+}]) or a low ratio (low intracellular [Ca^{2+}]). Percentage of cells with high intracellular calcium concentration is plotted for each time point. *C,* cell permeability of Ad5-infected and AdE3/19K-445A–infected CAF1 cells. *D,* viral release and production of Ad5, AdT1, and AdE3/19K-445A in the presence or absence of extracellular Ca^{2+} in carcinoma-associated fibroblasts. After infection, cells were incubated in normal or Ca^{2+}-free medium, and extracellular and intracellular viral contents were measured 48 h postinfection.

injected with AdT1 showed a more diffuse staining compared with Ad5, suggesting an improved spread of E3/19K-445A mutant virus (Fig. 6*D*).

Discussion

Improving the antitumor potency of current oncolytic adenoviruses represents one of the major challenges to obtain systemic therapeutic effect in clinical trials. Bioselection of randomly mutagenized pools of human Ad5 by repeated passaging under a predefined set of conditions is a classic virology strategy that has been recently postulated as a powerful method to develop more potent adenoviruses (18, 19). We hypothesized that the passage of Ad5 random mutants in an *in vivo* murine model of human cancer would provide a selective pressure environment closer to human tumors in the clinical setting, where the presence of a three-dimensional tumor stroma, the host immune system, and the proliferating status of tumor cells differ from those encountered in *in vitro* cell cultures.

By using this approach, we have isolated a new mutant virus, AdT1, which displays an enhanced antitumor activity when injected systemically in mice carrying s.c. human tumors. *In vitro* characterization revealed that AdT1 displays a large-plaque phenotype, which correlates with an increased cytotoxicity and release of viral progeny after replication, and a total viral yield not modified with respect to Ad5. Interestingly, the phenotype is not restricted to the pancreatic tumors where the bioselection process was developed, but the increased progeny release is also evident in different tumor cell types, including melanoma, lung, head and neck, and colorectal adenocarcinomas. Previously described adenoviral mutants with large-plaque phenotype include mutants in E1B/19K, in which E1A-induced apoptosis is not blocked (39), and premature cell death may lead to a reduced viral production. On the other hand, mutants that overexpress the adenovirus death protein (14, 35) or that express COOH truncating forms of the i-leader protein (18, 19) also display large-plaque phenotype, improving viral release without affecting the total yield. A double strategy, including the generation of Ad5/AdT1 recombinants and complete genome sequencing, allowed us to conclude that the alteration responsible for the AdT1-phenotype was the insertion of one nucleotide in the E3/19K coding region (mutation E3/19K-445A), subsequently leading to the COOH truncation of the protein and loss of its ER retention signal. The E3/19K glycoprotein retains the class I MHC heavy chain in the ER (40, 41) and prevents tapasin processing of class I MHC-bound peptides (33). However, to date, it has never been postulated as capable of modifying viral cycle kinetics and its functions are assumed to be nonessential for adenovirus growth *in vitro* (42), which has led to its deletion in many oncolytic adenoviruses (2).

Our studies show that the translocation of E3/19K-445A to the plasma membrane is the determinant for the enhanced release phenotype of AdT1 and AdE3/19K-445A. Other mutants that also

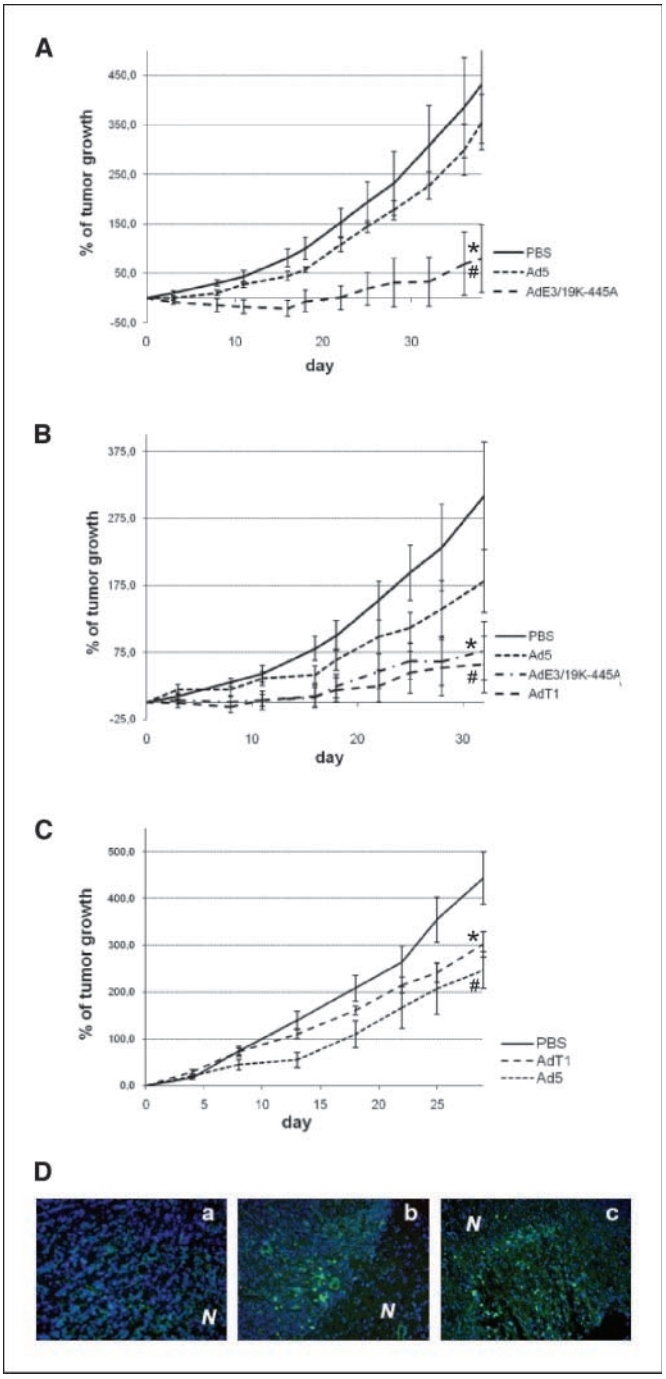

Figure 6. *In vivo* efficacy. *A,* NP-9 s.c. tumor xenografts were treated i.v. with PBS, Ad5, or AdE3/19K-445A. *Points,* mean percentage of tumor growth (n = 10); *bars,* SE. #, significant (P = 0.03) compared with the group treated with PBS; *, significant (P = 0.008) compared with mice injected with Ad5. *B,* NP-9 tumor xenografts were treated intratumorally with PBS, Ad5, AdT1, or AdE3/19K-445A. #, significant (P = 0.003) compared with tumors injected with PBS; *, significant (P = 0.002) compared with tumors injected with PBS. *C,* Syrian hamsters with s.c. HP-1 tumors were treated intratumorally with PBS, Ad5, or AdT1. *Columns,* mean percentage of tumor growth (n = 10); *bars,* SE. #, significant (P = 0.01) compared with tumors injected with PBS; *, significant (P = 0.04) compared with tumors injected with PBS. *D,* adenovirus intratumoral replication assessed by adenovirus detection in HP-1 pancreatic tumors grown s.c. in immunocompetent hamsters. Frozen sections of tumors obtained at day 29 after intratumoral injection of PBS (*a*), or 2.5×10^{10} vp of Ad5 (*b*) or AdT1 mutant (*c*) were treated with an anti-adenovirus antibody and counterstained with 4′,6′-diaminidino-2-phenylindole (×200). Sections taken from tumors treated with AdT1 displayed a more diffuse staining for adenovirus presence compared with Ad5-injected ones (*green dots*). *N,* necrotic areas.

induce a change of localization of E3/19K to the cell membrane by different genetic alterations, such as AdE3/19K-KS, also phenocopy the enhanced release of AdT1. This rules out the possibility that the precise E3/19K-445A alteration provokes a change in the complex splicing balance of the E3 region, leading to differential expression of ADP and enhanced cell death, as found with other E3 mutants (36). In fact, analysis of E3-specific mRNAs does not suggest any imbalance between the levels of the different transcripts after AdT1 infection with respect to Ad5. Furthermore, protein levels of ADP, E1A, and major structural proteins are not modified in E3/19K-445A containing adenoviruses. Overall, these data suggest that the viral cycle of AdT1 is only affected in its latest events, i.e., the plasma membrane permeabilization and the mutant virion release.

How E3/19K-445A relocalization improves adenovirus release is not clear at the present. This function is not related to the ability of E3/19K to bind MHC-I, its canonical target, but the presence of the mutation confers the protein the ability to initiate a new pathway. Apoptosis induction seems not to be the basis of the enhanced spreading of the E3/19K-445A mutants, as is the case for other large-plaque mutant adenoviruses (39). Interestingly, our results provide evidence that infection with E3/19K-445A expressing adenoviruses disrupts intracellular Ca^{2+} gradients maintained by the plasma and ER membranes, leading to an increase in the cytoplasmic calcium levels. Furthermore, the requirement for extracellular Ca^{2+} availability for the enhanced release phenotype of AdT1 suggests that such increases in intracellular calcium are due, at least in part, to the influx of extracellular calcium. Increases in intracellular calcium have been shown to be involved in animal virus-induced cytophatic effects and cell killing (43). Protein 2B from coxsackievirus, a protein with viroporin function, gradually induces the influx of extracellular Ca^{2+}, and release of Ca^{2+} from ER stores to permeabilize the plasma membrane and ultimately cause membrane lesions that allow the release of virus progeny (38). Interestingly, wild-type E3/19K is capable of mobilizing the ER pool of Ca^{2+} through an indirect mechanism (29). Although a direct role in Ca^{2+} mobilization by E3/19K-445A warrants experiments with the protein being autonomously expressed, we hypothesize that the mutant E3/19K acts functionally as a viroporin. Viroporins are nonessential, virally encoded, small membrane proteins that form selective channels in membranes, allowing the diffusion of ions and small molecules. Their deletion affects mainly the assembly and exit of virions (37). Their functions are related to both the modification of cell permeability to ions and membrane destabilization. The use of viroporins to promote progeny release is common to several families of viruses, such as picornavirus (38, 44), retrovirus (45), and orthomyxoviruses (46). In this context, our results suggest that, as a consequence of the selective pressure exerted in human xenografted tumors *in vivo*, adenovirus has evolved to incorporate an alternative and more efficient mechanism of release, which it lacks in its native form (where it uses ADP as the main mechanism), but that other animal viruses have previously selected. Moreover, the fact that the mutation selected in the current adenovirus bioselection process affects one of the main limitations found in oncolytic viruses suggests that pressure encountered in the environment of human tumors *in vivo* may be particularly relevant. Curiously, the latter stages in the viral cycle seem to be more prone to optimization within the tumor milieu. Further insight into the mechanism of release of E3/19K-COOH terminal truncated mutants could provide additional clues to understand the poorly characterized mechanism of release of native adenovirus modulation.

In terms of the immune response modulation, the E3/19K-445A form differs from its wild-type counterpart in its ability to bind and retain MHC class I molecules, but it is expected to retain the tapasin inhibition ability that wild-type E3/19K possesses. Mutants with truncated COOH terminal forms of the protein showed the ability to delay by 10-fold the maturation of class I molecules because they are still able to interact with TAP and interfere with tapasin function (33), and T1 mutants should behave similarly. More recently, it has been reported that E3/19K is additionally involved in evasion of natural killer (NK) cell recognition through its ability to interact with MHC-I chain–related proteins A and B (47). Although such function is impaired for E3/19K-445A protein, enhanced antitumoral activity of AdE3/19K-445A mutants obtained in different *in vivo* models in mice, where NK function is present, suggest that the lack of such function can be efficiently by-passed, at least in the particular environment associated to tumors. Further experiments in more immunocompetent models are necessary to establish the exact immunologic implications associated with the presence of the 445A mutation.

Transcription of E3 proteins is mainly regulated by E1A expression through ATF and AP-1 boxes within the E3 promoter (48), implying that the enhanced release phenotype associated with the expression of the mutant version of E3/19K is restricted to cells where E1A activation is permitted. We are currently generating conditional replicating adenoviruses that include the E3/19K-445A protein in the backbone of tumor promoter–driven E1A-regulated adenoviruses, such as ICOVIR-5 (11, 49), with the aim of increasing its ability to spread intratumorally. Interestingly, the increase in progeny release of AdT1 and AdE3/19K-445A mutants is specially noted in cancer-associated fibroblasts, a perpetually activated fibroblast population within desmoplastic lesions that are associated with malignant tumors (50). The release of E3/19K-445A mutant progeny occurs 3 days earlier with respect to that of Ad5 in the same cell population. Tumor stroma, composed of the extracellular matrix and mesenchymal cells, has been considered as a barrier to the efficient intratumoral diffusion of viruses (11, 12). Although the ability of oncolytic viruses to replicate in tumor-associated fibroblasts will depend on the selectivity mechanism in which the virus is based, the proliferative status of such fibroblasts (51) should allow efficient replication of pRB-dependent adenoviruses and the inclusion of E3/19K-445A mutation in ICOVIR-5 would provide the virus the ability to bypass fibroblast-mediated barriers.

Disclosure of Potential Conflicts of Interest

No potential conflicts of interest were disclosed.

Acknowledgments

Received 3/26/2008; revised 7/25/2008; accepted 8/25/2008.

Grant support: Mutua Madrileña Medical Research Foundation (Spain), Departament d'Universitats, Recerca i Societat de la Informació from Generalitat de Catalunya grant 2005 SGR 00727, and European Union 6th framework project research contract 18700 (Theradpox; R. Alemany). R. Alemany belongs to the Network of Cooperative Research on Cancer (C03-10), Instituto de Salud Carlos III of the Ministerio de Sanidad y Consumo, Government of Spain.

The costs of publication of this article were defrayed in part by the payment of page charges. This article must therefore be hereby marked *advertisement* in accordance with 18 U.S.C. Section 1734 solely to indicate this fact.

We thank Eduard Serra, Blanca Luena for her technical assistance in animal experiments, Dr. J.W. Yewdell (Laboratory of Viral Diseases, NIAID, NIH) and Dr. W.S.M Wold (St. Louis University) for providing Tw1.3. and anti-ADP antibodies, respectively, and Lynda Coughlan for the extensive revision of this manuscript.

References

1. Liu TC, Galanis E, Kirn D. Clinical trial results with oncolytic virotherapy: a century of promise, a decade of progress. Nat Clin Pract Oncol 2007;4:101–17.
2. Alemany R. Cancer selective adenoviruses. Mol Aspects Med 2007;28:42–58.
3. Aghi M, Martuza RL. Oncolytic viral therapies - the clinical experience. Oncogene 2005;24:7802–16.
4. Chu RL, Post DE, Khuri FR, Van Meir EG. Use of replicating oncolytic adenoviruses in combination therapy for cancer. Clin Cancer Res 2004;10:5299–312.
5. Hamid O, Varterasian ML, Wadler S, et al. Phase II trial of intravenous CI-1042 in patients with metastatic colorectal cancer. J Clin Oncol 2003;21:1498–504.
6. Small EJ, Carducci MA, Burke JM, et al. A phase I trial of intravenous CG7870, a replication-selective, prostate-specific antigen-targeted oncolytic adenovirus, for the treatment of hormone-refractory, metastatic prostate cancer. Mol Ther 2006;14:107–17.
7. Alemany R, Suzuki K, Curiel DT. Blood clearance rates of adenovirus type 5 in mice. J Gen Virol 2000;81:2605–9.
8. Bernt KM, Ni S, Gaggar A, et al. The effect of sequestration by nontarget tissues on anti-tumor efficacy of systemically applied, conditionally replicating adenovirus vectors. Mol Ther 2003;8:746–55.
9. Muruve DA. The innate immune response to adenovirus vectors. Hum Gene Ther 2004;15:1157–66.
10. Wilson JM. Adenoviruses as gene-delivery vehicles. N Engl J Med 1996;334:1185–7.
11. Cascallo M, Alonso MM, Rojas JJ, et al. Systemic toxicity-efficacy profile of ICOVIR-5, a potent and selective oncolytic adenovirus based on the pRB pathway. Mol Ther 2007;15:1607–15.
12. Sauthoff H, Hu J, Maca C, et al. Intratumoral spread of wild-type adenovirus is limited after local injection of human xenograft tumors: virus persists and spreads systemically at late time points. Hum Gene Ther 2003;14:425–33.
13. Wein LM, Wu JT, Kirn DH. Validation and analysis of a mathematical model of a replication-competent oncolytic virus for cancer treatment: implications for virus design and delivery. Cancer Res 2003;63:1317–24.
14. Doronin K, Toth K, Kuppuswamy M, et al. Tumor-specific, replication-competent adenovirus vectors overexpressing the adenovirus death protein. J Virol 2000;74:6147–55.
15. van Beusechem VW, van den Doel PB, Grill J, Pinedo HM, Gerritsen WR. Conditionally replicative adenovirus expressing p53 exhibits enhanced oncolytic potency. Cancer Res 2002;62:6165–71.
16. Wildner O, Blaese RM, Morris JC. Therapy of colon cancer with oncolytic adenovirus is enhanced by the addition of herpes simplex virus-thymidine kinase. Cancer Res 1999;59:410–3.
17. Bristol JA, Zhu M, Ji H, et al. *In vitro* and *in vivo* activities of an oncolytic adenoviral vector designed to express GM-CSF. Mol Ther 2003;7:755–64.
18. Yan W, Kitzes G, Dormishian F, et al. Developing novel oncolytic adenoviruses through bioselection. J Virol 2003;77:2640–50.
19. Subramanian T, Vijayalingam S, Chinnadurai G. Genetic identification of adenovirus type 5 genes that influence viral spread. J Virol 2006;80:2000–12.
20. Villanueva A, Garcia C, Paules AB, et al. Disruption of the antiproliferative TGF-β signaling pathways in human pancreatic cancer cells. Oncogene 1998;17:1969–78.
21. Batra SK, Metzgar RS, Worlock AJ, Hollingsworth MA. Expression of the human MUC1 mucin cDNA in a hamster pancreatic tumor cell line HP-1. Int J Pancreatol 1992;12:271–83.
22. Alemany R, Curiel DT. CAR-binding ablation does not change biodistribution and toxicity of adenoviral vectors. Gene Ther 2001;8:1347–53.
23. Williams JF, Gharpure M, Ustacelebi S, McDonald S. Isolation of temperature-sensitive mutants of adenovirus type 5. J Gen Virol 1971;11:95–101.
24. Cascallo M, Gros A, Bayo N, et al. Deletion of VAI and VAII RNA genes in the design of oncolytic adenoviruses. Hum Gene Ther 2006;17:929–40.
25. Cox JH, Bennink JR, Yewdell JW. Retention of adenovirus E19 glycoprotein in the endoplasmic reticulum is essential to its ability to block antigen presentation. J Exp Med 1991;174:1629–37.
26. Tollefson AE, Scaria A, Saha SK, Wold WS. The 11,600-MW protein encoded by region E3 of adenovirus is expressed early but is greatly amplified at late stages of infection. J Virol 1992;66:3633–42.
27. Burchiel SW, Edwards BS, Kuckuck FW, et al. Analysis of free intracellular calcium by flow cytometry: multiparameter and pharmacologic applications. Methods 2000;21:221–30.
28. Jackson MR, Nilsson T, Peterson PA. Retrieval of transmembrane proteins to the endoplasmic reticulum. J Cell Biol 1993;121:317–33.
29. Pahl HL, Sester M, Burgert HG, Baeuerle PA. Activation of transcription factor NF-κB by the adenovirus E3/19K protein requires its ER retention. J Cell Biol 1996;132:511–22.
30. Tollefson AE, Ryerse JS, Scaria A, Hermiston TW, Wold WS. The E3–11.6-kDa adenovirus death protein (ADP) is required for efficient cell death: characterization of cells infected with adp mutants. Virology 1996;220:152–62.
31. Hermiston TW, Tripp RA, Sparer T, Gooding LR, Wold WS. Deletion mutation analysis of the adenovirus type 2 E3–19K protein: identification of sequences within the endoplasmic reticulum lumenal domain that are required for class I antigen binding and protection from adenovirus-specific cytotoxic T lymphocytes. J Virol 1993;67:5289–98.
32. Sester M, Burgert HG. Conserved cysteine residues within the E3/19K protein of adenovirus type 2 are

essential for binding to major histocompatibility complex antigens. J Virol 1994;68:5423–32.
33. Bennett EM, Bennink JR, Yewdell JW, Brodsky FM. Cutting edge: adenovirus E19 has two mechanisms for affecting class I MHC expression. J Immunol 1999;162: 5049–52.
34. White E, Grodzicker T, Stillman BW. Mutations in the gene encoding the adenovirus early region 1B 19,000-molecular-weight tumor antigen cause the degradation of chromosomal DNA. J Virol 1984;52: 410–9.
35. Tollefson AE, Scaria A, Ying B, Wold WS. Mutations within the ADP (E3-11.6K) protein alter processing and localization of ADP and the kinetics of cell lysis of adenovirus-infected cells. J Virol 2003; 77:7764–78.
36. Scaria A, Wold WS. Fine-mapping of sequences that suppress splicing in the E3 complex transcription unit of adenovirus. Virology 1994;205:406–16.
37. Gonzalez ME, Carrasco L. Viroporins. FEBS Lett 2003;552:28–34.
38. van Kuppeveld FJ, Hoenderop JG, Smeets RL, et al. Coxsackievirus protein 2B modifies endoplasmic reticulum membrane and plasma membrane permeability and facilitates virus release. EMBO J 1997;16: 3519–32.
39. Pilder S, Logan J, Shenk T. Deletion of the gene encoding the adenovirus 5 early region 1b 21,000-molecular-weight polypeptide leads to degradation of viral and host cell DNA. J Virol 1984;52:664–71.
40. Andersson M, Paabo S, Nilsson T, Peterson PA. Impaired intracellular transport of class I MHC antigens as a possible means for adenoviruses to evade immune surveillance. Cell 1985;43:215–22.
41. Burgert HG, Kvist S. An adenovirus type 2 glycoprotein blocks cell surface expression of human histocompatibility class I antigens. Cell 1985;41:987–97.
42. Bhat BM, Wold WS. A small deletion distant from a splice or polyadenylation site dramatically alters pre-mRNA processing in region E3 of adenovirus. J Virol 1987;61:3938–45.
43. Chami M, Oules B, Paterlini-Brechot P. Cytobiological consequences of calcium-signaling alterations induced by human viral proteins. Biochim Biophys Acta 2006;1763:1344–62.
44. de Jong AS, Schrama IW, Willems PH, et al. Multimerization reactions of coxsackievirus proteins 2B, 2C and 2BC: a mammalian two-hybrid analysis. J Gen Virol 2002;83:783–93.
45. Gonzalez ME, Carrasco L. The human immunodeficiency virus type 1 Vpu protein enhances membrane permeability. Biochemistry 1998;37:13710–9.
46. Guinea R, Carrasco L. Influenza virus M2 protein modifies membrane permeability in E. coli cells. FEBS Lett 1994;343:242–6.
47. McSharry BP, Burgert HG, Owen DP, et al. Adenovirus E3/19K promotes evasion of NK cell recognition by intracellular sequestration of the NKG2D ligands major histocompatibility complex class I chain-related proteins A and B. J Virol 2008;82:4585–94.
48. Akusjarvi G. Proteins with transcription regulatory properties encoded by human adenoviruses. Trends Microbiol 1993;1:163–70.
49. Alonso MM, Cascallo M, Gomez-Manzano C, et al. ICOVIR-5 shows E2F1 addiction and potent antiglioma effect *in vivo*. Cancer Res 2007;67:8255–63.
50. Kalluri R, Zeisberg M. Fibroblasts in cancer. Nat Rev Cancer 2006;6:392–401.
51. Hasebe T, Sasaki S, Imoto S, Ochiai A. Proliferative activity of intratumoral fibroblasts is closely correlated with lymph node and distant organ metastases of invasive ductal carcinoma of the breast. Am J Pathol 2000;156:1701–10.